

### Supplementary Fig. 1: B7-H4 in breast cancer cells promotes tumor progression.

**a** Schematic diagram shows the generation of a 4H11 clone that expresses endogenous B7-H4 from the MPA-DMBA tumor model. MPA, medroxyprogesterone acetate. DMBA, 7, 12-dimethylbenz[a]anthracene.

**b** Immunoblot for B7-H4 in 4H11 control (WT) and B7-H4 knockout (KO) cells.

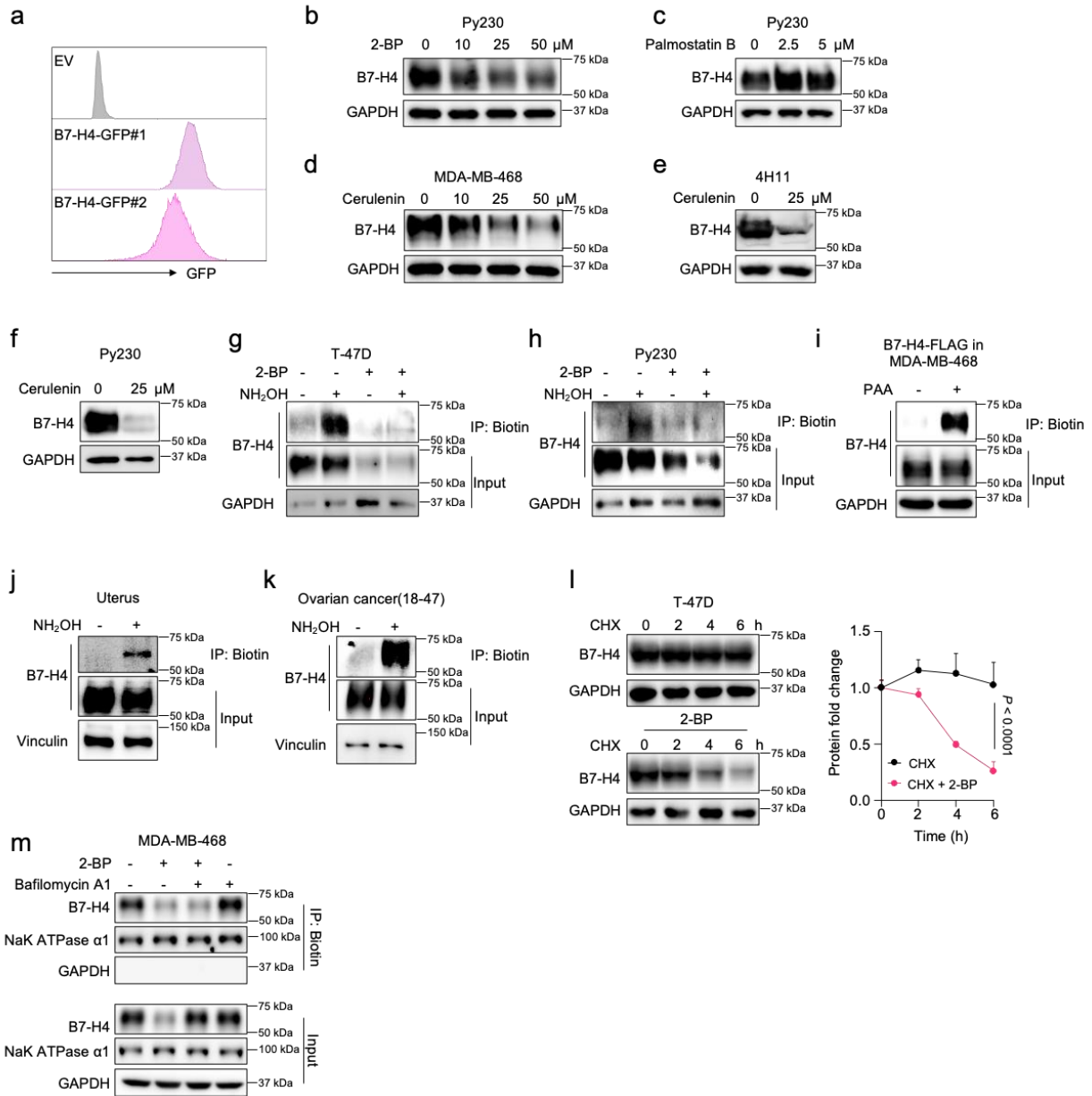
**c** In vitro cell proliferation assay for WT and KO 4H11 cells from three independent tests. Data are shown as mean  $\pm$  SEM. Statistical analysis was performed using two-way ANOVA.

**d** Tumor weights of B7-H4 KO (n = 10 in C57BL/6 mice and n = 8 in NSG mice) and WT (n = 9 in C57BL/6 mice and n = 7 in NSG mice) 4H11 tumors in immune-competent and NSG mice. Pooled data from 2 independent experiments. Subcutaneous implantation was conducted in 10-week-old female C57BL/6 or NSG mice. Data are shown as mean  $\pm$  SEM. Statistical analysis was performed using one-way ANOVA with Tukey's multiple comparison test.

**e** Flow cytometry analysis of tumor-infiltrating CD8<sup>+</sup> T cells in subcutaneous 4H11 WT (n = 18) and B7-H4-KO (n = 13) tumor-bearing mice. 4H11 tumor-bearing mice. Pooled data from 2 independent experiments. Subcutaneous implantation was conducted in 10-week-old female C57BL/6 mice. Data are shown as mean  $\pm$  SEM. Statistical analysis was performed using two-tailed Student's t test.

**f** Immunoblot for B7-H4 overexpression in 4T1 cells.

Source data are provided as Source Data File.



## Supplementary Fig. 2: B7-H4 palmitoylation prevents its lysosomal degradation.

**a** Representative image of flow cytometry detection of two B7-H4-GFP expressing clones isolated from MDA-MB-468 cells.

**b,c** Immunoblot for B7-H4 in Py230 cells treated with 2-BP (**b**) or palmostatin B (**c**) at the indicated concentrations for 24 hours.

**d-f** Immunoblot for B7-H4 in MDA-MB-468 (**d**), 4H11 (**e**), and Py230 (**f**) cells treated with cerulenin at the indicated concentrations for 24 hours.

**g,h** Endogenous B7-H4 palmitoylation in T-47D (**g**) and Py230 (**h**) cells treated with or without (w/o) 2-BP (100  $\mu$ M) determined by ABE assay.

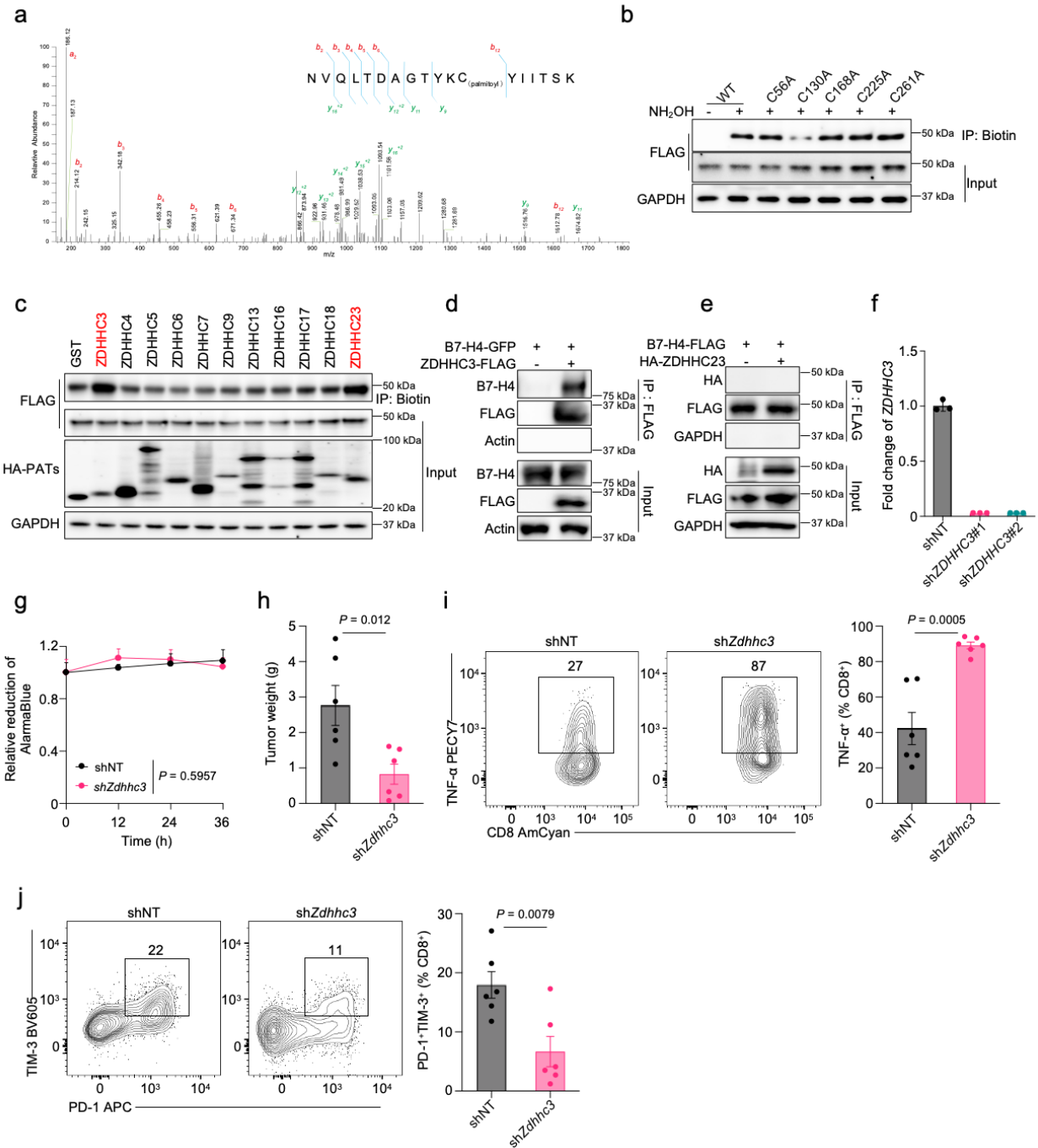
**i** Palmitoylation of B7-H4 overexpressed in MDA-MB-468 cells determined by Click-iT assay. PAA, 15-azidopentadecanoic acid.

**j,k** Biotin-acyl-exchange (ABE) detects endogenous B7-H4 palmitoylation in normal mouse uterine (**j**) and human ovarian cancer (**k**) tissues.

**l** Representative immunoblot for B7-H4 and protein level quantification from three independent tests in T-47D cells examined by cycloheximide (CHX) chase assay w/o 2-BP (100  $\mu$ M). Data are shown as mean  $\pm$  SEM. Statistical analyses were performed using two-way ANOVA with Sidak's multiple comparisons test.

**m** Immunoblot for cell surface B7-H4 in MDA-MB-468 cells treated with 2-BP (50  $\mu$ M) and/or bafilomycin A1 (100 nM) for 24 hours.

Source data are provided as Source Data File.



**Supplementary Fig. 3: ZDHHC3 catalyzes B7-H4 palmitoylation at Cys130 impairing tumor immunity.**

**a** Mass spectrometry identifies B7-H4 palmitoylation at Cys130.

**b** Palmitoylation of B7-H4 mutants in 293T cells detected by ABE assay.

**c** Representative immunoblot for screening palmitoyltransferase of B7-H4 by ABE assay.

**d** Interaction between B7-H4-GFP and ZDHHC3-Flag in 293T cells.

**e** Co-immunoprecipitation to detect the possible interaction between B7-H4 and ZDHHC23 in 293T cells.

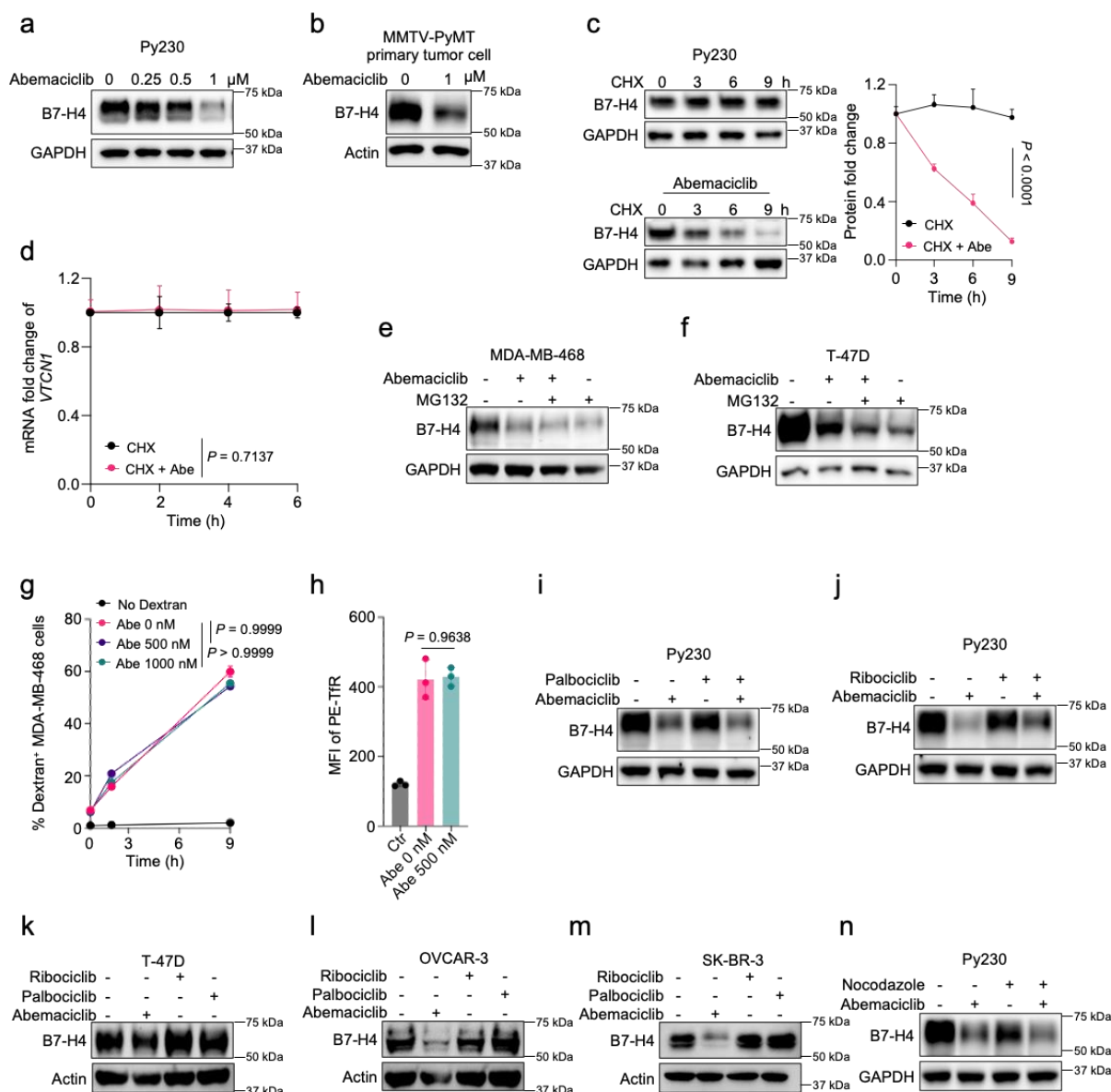
**f** mRNA levels of ZDHHC3 in T-47D ZDHHC3 knockdown cells. Data are shown as mean  $\pm$  SD.

**g** In vitro cell proliferation of control (shNT, non-targeting shRNA) and *Zdhhc3* knockdown 4H11 cells from three independent tests. Data are shown as mean  $\pm$  SEM. Statistical analysis was performed using two-way ANOVA with Sidak's multiple comparisons test.

**h** *Zdhhc3* knockdown (sh*Zdhhc3*) and control (shNT) 4H11 subcutaneous tumor weights. n = 6 per group. Subcutaneous implantation was conducted in 8-week-old female C57BL/6 mice. Data are shown as mean  $\pm$  SEM. Statistical analysis was performed using two-way ANOVA with Sidak's multiple comparisons test.

**i,j** Flow cytometry analysis of tumor-infiltrating TNF- $\alpha$ <sup>+</sup> (i) and PD-1<sup>+</sup>TIM-3<sup>+</sup> (j) CD8<sup>+</sup> T cells in subcutaneous 4H11 tumor-bearing mice. n = 6 per group. Subcutaneous implantation was conducted in 8-week-old female C57BL/6 mice. Data are shown as mean  $\pm$  SEM. Statistical analyses were performed using two-tailed Student's t test.

Source data are provided as Source Data File.



**Supplementary Fig. 4: Abemaciclib promotes B7-H4 lysosomal degradation.**

**a,b** Immunoblot for B7-H4 in Py230 (**a**) and MMTV-PyMT (**b**) breast cancer cells treated with abemaciclib at the indicated concentrations for 24 hours.

**c** Representative immunoblot for B7-H4 and protein level quantification from three independent tests in Py230 cells examined by cycloheximide (CHX) chase assay combined w/o abemaciclib (1  $\mu$ M) treatment. Data are shown as mean  $\pm$  SEM. Statistical analysis was performed using two-way ANOVA with Sidak's multiple comparisons test.

**d** mRNA fold change of B7-H4 in MDA-MB-468 cells in the setup of Fig. 4g. Data are shown as mean  $\pm$  SD. Statistical analysis was performed using two-way ANOVA with Sidak's multiple comparisons test.

**e,f** Immunoblot for B7-H4 in MDA-MB-468 (**e**) and T-47D (**f**) cells treated with abemaciclib (1  $\mu$ M) and/or MG132 (100 nM) for 24 hours.

**g,h** The uptake of FITC-Dextran (100  $\mu$ g/mL) and the mean fluorescence intensity (MFI) of the surface transferrin receptor (TfR) in MDA-MB-468 cells treated with or without abemaciclib at the indicated concentrations for 20 hours. n = 3 per group. Data are presented as mean  $\pm$  SD. Statistical analyses were conducted using two-way ANOVA (**g**) and one-way ANOVA with Dunnett's multiple comparisons test (**h**).

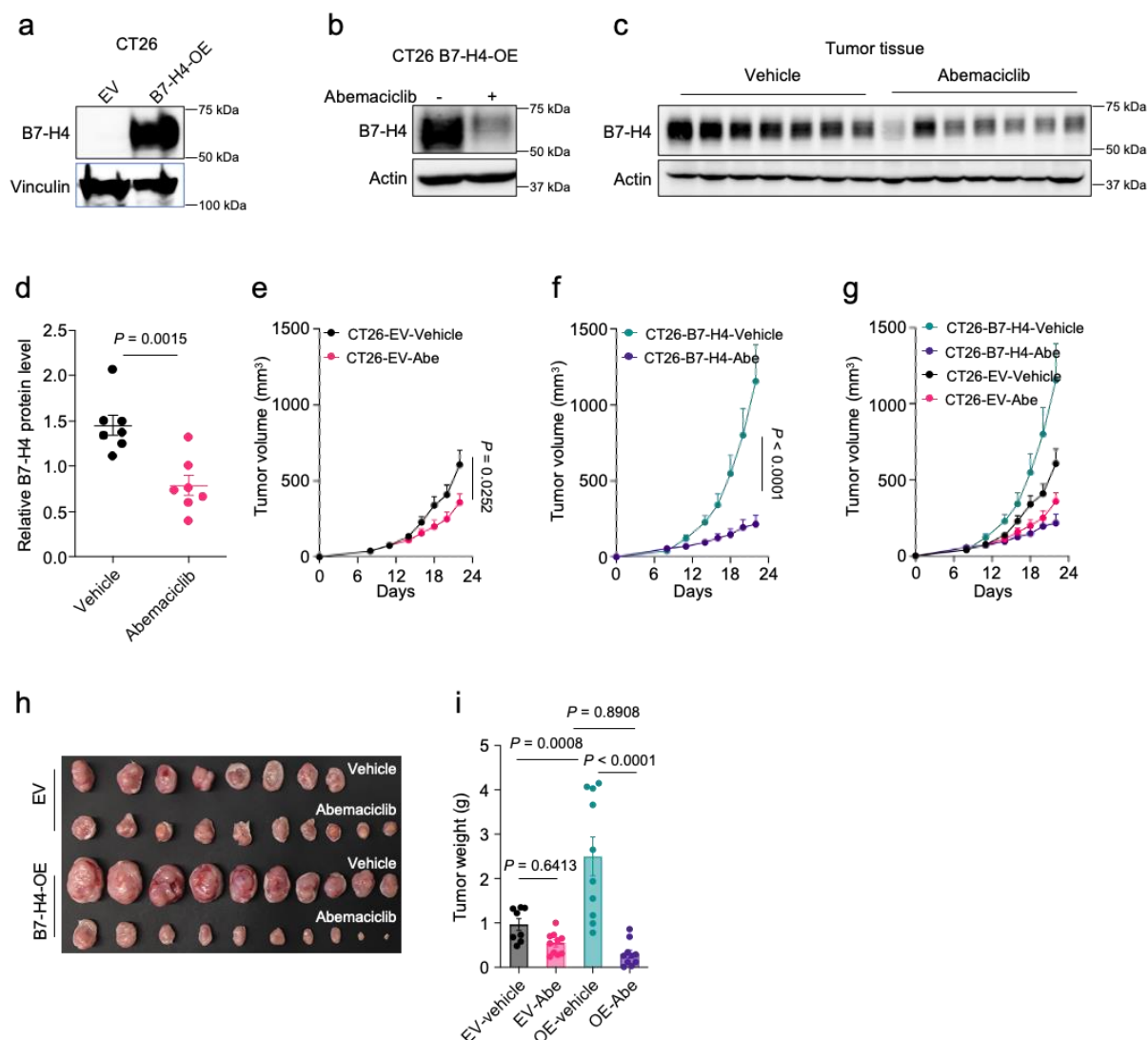
**i,j** Immunoblot for B7-H4 in Py230 cells treated with abemeciclib (1  $\mu$ M) and/or palbociclib (1  $\mu$ M) (**i**) and ribociclib (1  $\mu$ M) (**j**) for 24 hours.

**k-m** Immunoblot for B7-H4 in SK-BR-3 (**k**), T-47D (**l**), and OVCAR-3 (**m**) cells treated with abemeciclib (1  $\mu$ M), palbociclib (1  $\mu$ M), or ribociclib (1  $\mu$ M) respectively.

**n** Immunoblot for B7-H4 in Py230 cells treated with abemeciclib (1  $\mu$ M) and/or nocodazole (1  $\mu$ M) for 24 hours.

Source data are provided as Source Data File.





**Supplementary Fig. 5: Abemaciclib enhances B7-H4 lysosomal degradation promoting tumor immunity.**

**a,b** Immunoblot for B7-H4 in B7-H4 overexpressing (B7-H4-OE) CT26 cells (**a**) and in B7-H4-OE CT26 cells treated with abemaciclib (1  $\mu$ M) for 24 hours (**b**).

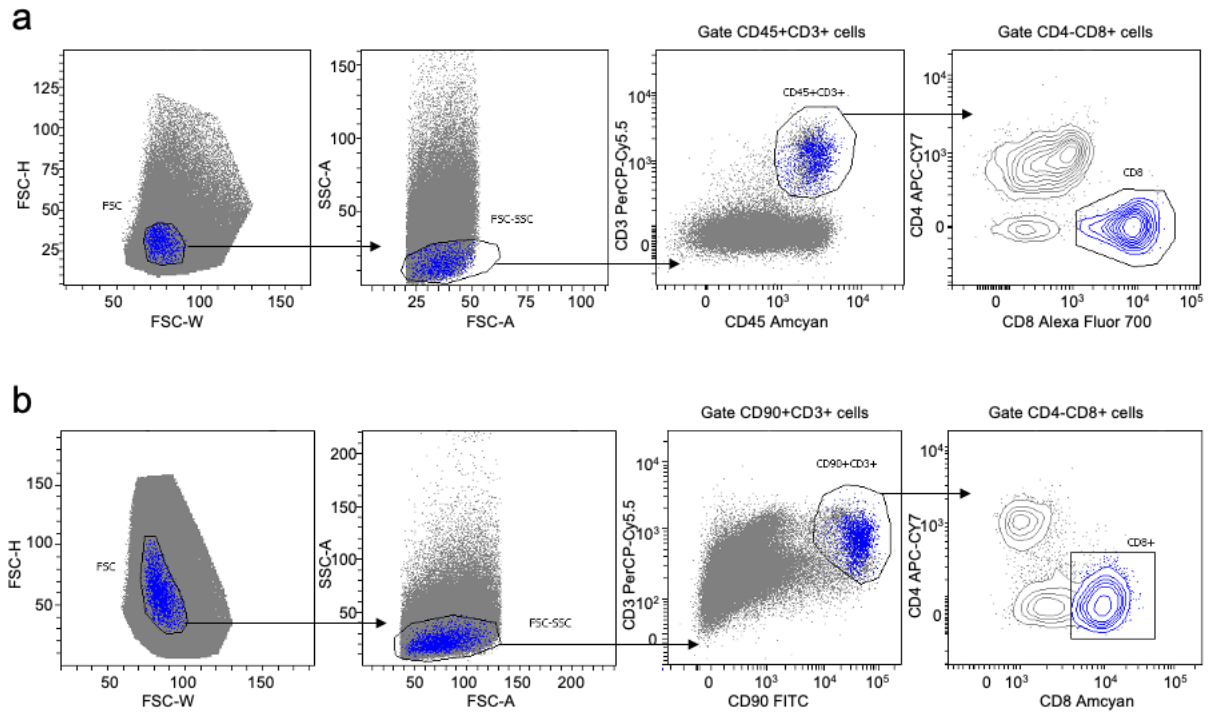
**c,d** Immunoblot (**c**) and quantification (**d**) for B7-H4 in primary tumor cells isolated from CT-26-B7-H4 tumor-bearing mice treated with vehicle or abemaciclib (75 mg/kg, every two days).  $n = 7$  per group. Subcutaneous implantation was conducted in 8-week-old female C57BL/6 mice. Data are shown as mean  $\pm$  SEM (**d**). Statistical analysis was conducted using two-tailed Student's  $t$  test.

**e-g** CT26-EV ( $n = 8$  for vehicle and  $n = 10$  for abemaciclib group) (**e**), or CT26-B7-H4 ( $n = 10$  for vehicle and abemaciclib) (**f**) subcutaneous tumor growth in mice treated with vehicle or abemaciclib (75 mg/kg, every two days), and the combined growth curves (**g**).

Subcutaneous implantation was conducted in 8-week-old female C57BL/6 mice. Data are shown as mean  $\pm$  SEM. Statistical analyses were conducted using two-way ANOVA (**e,f**).

**h,i** Representative image (**h**) and tumor weights (**i**) of B7-H4-OE (n = 10 for vehicle and abemaciclib) and empty vector (EV) (n = 8 for vehicle and n = 10 for abemaciclib group) harboring CT26 subcutaneous tumors in mice treated with vehicle or abemaciclib (75 mg/kg, every two days). Subcutaneous implantation was conducted in 8-week-old female C57BL/6 mice. Data are shown as mean  $\pm$  SEM. Statistical analyses were conducted using one-way ANOVA with Tukey's multiple comparison test.

Source data are provided as Source Data File.



**Supplementary Fig. 6: Gating strategies for flow cytometry of tumor-infiltrating CD8<sup>+</sup> T cells.**

**a** Gating strategy used to gate CD8<sup>+</sup> T cells from single-cell suspensions of the indicated tumor tissues. This strategy was applied for cell surface staining with cell-specific markers in Fig. 1d, e, k, o, and Supplementary Fig. 3j.

**b** Gating strategy used to gate CD8<sup>+</sup> T cells for measuring intracellular cytokine staining in Fig. 1c, 3n, and Supplementary Fig. 3i.

FSC-A: Forward scatter area; FSC-H: Forward scatter height; FSC-W: Forward scatter width; SSC-A: Side scatter area; PerCP-Cy5.5: Peridinin-Chlorophyll-protein-Cyanine5.5; FITC: Fluorescein isothiocyanate.